RSC Advances

ROYAL SOCIETY OF CHEMISTRY

www.rsc.org/advances

View Article Online
DOI: 10.1039/C5RA08819D

Graphical Abstract

Polymer chip-integrable piezoelectric micropump with low backpressure dependence

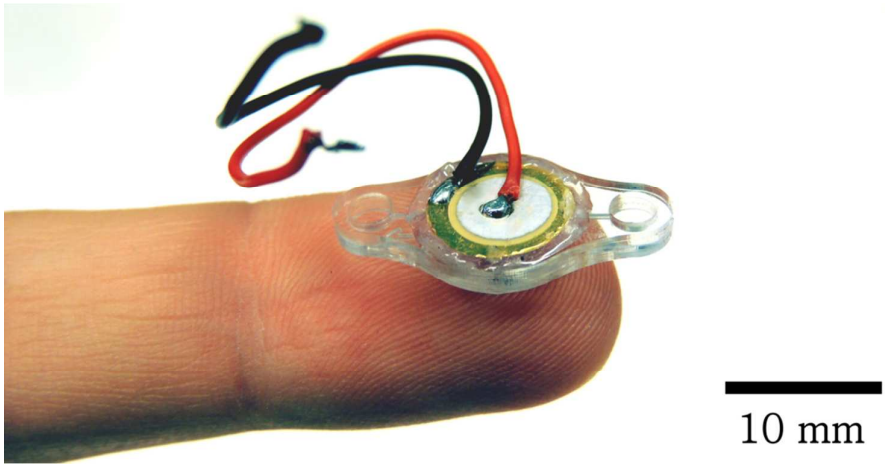

A polymer piezoelectric micropump fabricated with conventional machining methods that can be embedded in laminated microfluidic chips

View Article Online
DOI: 10.1039/C5RA08819D

RSC Advances

COMMUNICATION

Polymer chip-integrable piezoelectric micropump with low backpressure dependence†

Received 00th January 20xx,
Accepted 00th January 20xx

DOI: 10.1039/x0xx00000x

www.rsc.org/

A.J. Conde,‡[a] A. Bianchetti,[b] F.E. Veiras,[b,c] A. Federico,[b] J. M. Cabaleiro,[d] M. Dufva,[e] R. E. Madrid[f] and L. Fraigi[a]

We describe a piezoelectric micropump constructed in polymers with conventional machining methods. The micropump is self-contained and can be built as an independent device or as an on-chip module within laminated microfluidic chips. We demonstrate on-chip integrability by the fabrication and testing of an active micromixer with two pumps. Average flow rates from sub-µl min^{-1} to 300 µl min^{-1} can be obtained with low influence from the backpressure up to approximately 10 kPa. The micropump design allows potential use in low-cost disposable polymeric Lab on a Chip devices.

Micropumps are fundamental components in Lab on a Chip (LOC) devices; they control and modulate fluid flow within their microfluidic networks. Extensive research in the field of micropumps has been done and a large number of pumping mechanisms have been developed, most of them overviewed in comprehensive reviews published in the last years.[1-4] Among micropumps, the most studied by far are the so-called reciprocating displacement micropumps (RDµPs) normally featuring a pumping membrane and two passive valves for flow rectification. A typical characteristic of most academic and commercial RDµPs is that they suffer from backpressure-dependence of the flow rate in all their working range, usually decreasing linearly with increasing backpressure.[5-9] This inherent dependence can be a drawback for some applications such as drug delivery, microfluidic networks with unknown or varying hydrodynamic resistance or microfluidic systems having reservoirs, where height changes in the liquid columns induce fluctuating backpressures. Several RDµPs have been developed to deliver fluids independently of the varying outlet conditions, all of them based on silicon manufacturing.[10-13] The main drawbacks of these devices are the non-optical transparency of silicon, high associated costs and impossibility to integrate within the polymeric fabrication processes on which most LOC devices are based.[14] Furthermore, rapid prototyping is not possible in silicon-based devices.[15]

In this work, we describe the design, fabrication and characterization of a RDµP with low backpressure dependence completely constructed in transparent, low-cost polymers using conventional manufacturing methods. We developed a new simple method to integrate polydimethylsiloxane (PDMS) moving structures to form passive check valves within laminated polymethyl methacrylate (PMMA) LOC devices without the need of complex bonding techniques usually applied to PDMS/PMMA devices.[16-19] We have successfully used this method to fabricate on-chip RDµPs with low backpressure dependence at the same time with other microfluidic structures forming monolithic chips. We demonstrate this concept by the fabrication and testing of a well-known device in the microfluidics community, such as the sequential injection micromixer, featuring two independent micropumps within the same microfluidic chip.

Although with a different working principle, there is a previous report of a similar polymer piezoelectric micropump [20]. However, the flow rate in this device is strongly dependent on the outlet backpressure and some of its fabrication processes also require silicon manufacturing.

Design, fabrication and characterization

The micropump design is based on a layered construction (Fig. 1a) consisting of four structural layers: three machined PMMA (Clarex, Japan) layers (I to III in Fig. 1a) and a piezoelectric diaphragm (unimorph disc). The check valves are formed when custom-made flexible PDMS diaphragms (Fig. 1b) are sandwiched between appropriate structures fabricated in the PMMA layers. More detailed drawings of the pump

[a] Centro de Micro y Nanoelectrónica del Bicentenario (CMNB), Instituto Nacional de Tecnología Industrial (INTI). Av. Gral. Paz 5445, Edificio 42, San Martín, Buenos Aires, Argentina. E-mail: aconde85@gmail.com.
[b] Electrónica e Informática, INTI, San Martín, Buenos Aires, Argentina.
[c] Laboratorio de Sistemas Líquidos, GLOmAe, FIUBA, Argentina.
[d] Laboratorio de Fluidodinámica, FIUBA, Argentina / Laboratorio de Micro y Nanofluídica y Plasma, UdeMM, Argentina.
[e] DTU Nanotech, Technical University of Denmark, Denmark.
[f] Instituto Superior de Investigaciones Biológicas (INSIBIO-CONICET), Laboratorio de Medios e Interfases (LAMEIN), Dpto. de Bioingeniería FACET/UNT, Tucumán, Argentina
‡ Corresponding author.
† Electronic Supplementary Information (ESI) available: [Fig. S1 to S5 and supplementary movies 1 to 5]. See DOI: 10.1039/x0xx00000x

View Article Online
DOI: 10.1039/C5RA08819D

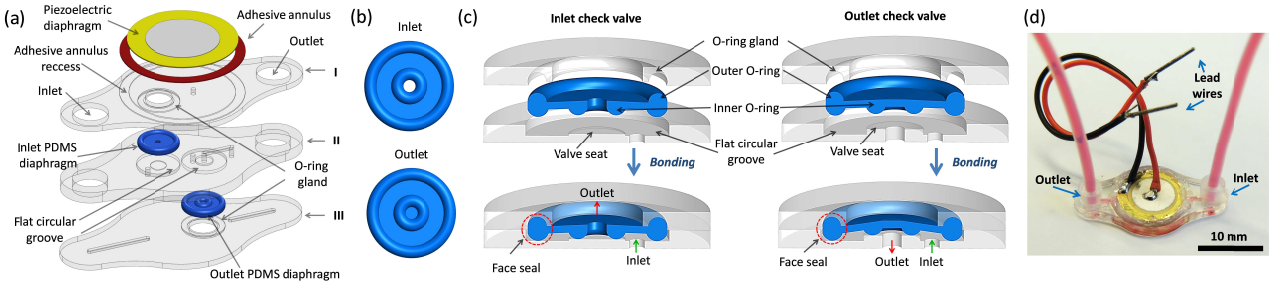

Fig. 1 (a) Exploded view of the micropump as an independent device. (b) Top view of the PDMS diaphragms. Inlet diaphragm has a hole in the centre of the inner O-ring while the outlet diaphragm does not. (c) Section view of the check valves showing the outer O-rings self-alignment, liquid tight seals formation and the coupling between the valve seats and the inner O-rings. The pretension applied to the outlet PDMS diaphragm is larger than the one applied to the inlet PDMS diaphragm. (e) Photograph of a fully-assembled independent micropump with tubing attached.

layers (and relevant structures) and the PDMS diaphragms are presented in Fig. S1.†

The working principle of the presented micropump is no different from a typical RDμP: the piezoelectric diaphragm alternately increases and decreases the pump chamber volume, which forces fluid in and out of the chamber in one direction due to the rectification of flow accomplished by the inlet and outlet check valves on each half cycle.[1] However, the design of the outlet check valve also limits the influence of the outlet pressure towards the pumping chamber -in a certain range- in the complete pump cycle, which yields the low backpressure dependence of the flow rate. This design has been previously reported[10] and is briefly explained in Fig. S2.† The inlet check valve is designed as a typical diaphragm check valve with a small cracking pressure.

The check valves have different designs but they share two common structural features.First, both inlet and outlet PDMS diaphragms are surrounded by tori (outer O-rings). The upper half of the outer O-rings fits and self-aligns (limiting lateral movement) in complementary half-round circular grooves (O-ring glands) fabricated in the PMMA layers (Fig. 1c). The lower half of the outer O-rings is slightly larger than the depth of the flat circular groove. Consequently, when the layers are bonded, the flat groove compresses and deforms the outer O-ring, which in turn compresses the upper half of the O-ring towards the rigid walls of the O-ring gland forming a face seal that produce gas- and liquid-tight closures (Fig. 1c). This seal can withstand pressures up to 50 kPa without measurable leakage. By using this approach, the PDMS diaphragms are also mechanically anchored to the PMMA structures when layers are bonded, thus avoiding any chemical assistance or surface functionalization. Second, both valve seats provide the rigid support for the half-tori (inner O-rings) that bulge out of the centre of both PDMS diaphragms (Fig. 1c). Pretension is applied to the diaphragms by regulating valve seat heights, which causes the inner O-rings to form a tight, but reversible, seal with the rigid valve seats. This seal puts both valves in a normally closed state that avoids unwanted leaking and is also closely related to the working mechanism of outlet check valve.

All the PMMA layers of the pump were fabricated *via* computer numerical control (CNC) micromilling following a procedure previously described.[21] Layers I and III are fabricated from a 0.5 mm thick PMMA sheet while layer II is fabricated from a 1 mm thick PMMA sheet. Inlet and outlet ports are designed to fit tubing with an adhesive-free and reusable interconnection.[22] All milling tools were purchased from Kyocera Microtools, USA. The diaphragms were fabricated by injection molding of PDMS in PMMA molds following the steps described in Fig. S3.†

The pump layers were laminated *via* a thermal UV-assisted bonding process following the same steps previously described.[21] Briefly, the pump layers were gently cleaned to remove debris, sonicated in isopropyl alcohol for 2 min, rinsed with deionized water and finally blown-dried with filtered air. The PDMS diaphragms were fitted in their corresponding O-ring gland just after the bonding faces of the layers were exposed to UV light (250 W quartz mercury lamp) for 1 min. The layers were stacked, fitted in an alignment frame and subsequently bonded between glass plates in a bonding press (Shimeq, Argentina) at 80 °C for 15 min with an applied pressure of 2 MPa. After bonding, a 9.5 mm diameter off-the-shelf piezoelectric diaphragm (Cold Gold Audio, Canada) is glued to layer I *via* an epoxy adhesive (Poxipol, Argentina) annulus that fits in a recess fabricated in layer I so as to diminish the dead volume of the pump chamber. The brass plate of the piezoelectric diaphragm works as the pumping membrane and it is in direct contact with the fluid. A photograph of the fully-assembled micropump with tubing attached is shown in Fig. 1d. More photographs of the bonded pump layers and a finished micropump can be found in Fig. S4.†

Experimental characterization of the micropump was accomplished by studying pump outlet characteristics -flow rate and pressure- as a function of parameters such as actuating voltage, actuating frequency and backpressure using the set-up and methods described in Fig. S5.† For all testing conditions, a 50% duty cycle square wave was used. Several micropumps were fabricated and tested (n=4) and the results averaged. Measurement error is around 5%.

The instantaneous velocity fields produced by the micropump in microfluidic channels were measured by micro-particle image velocimetry (μPIV) using a similar set-up as described by Devasenathipathy *et al.*[23] The obtained images were processed in analysis software DaVis (LaVision GmbH, Germany).

View Article Online
DOI: 10.1039/C5RA08819D

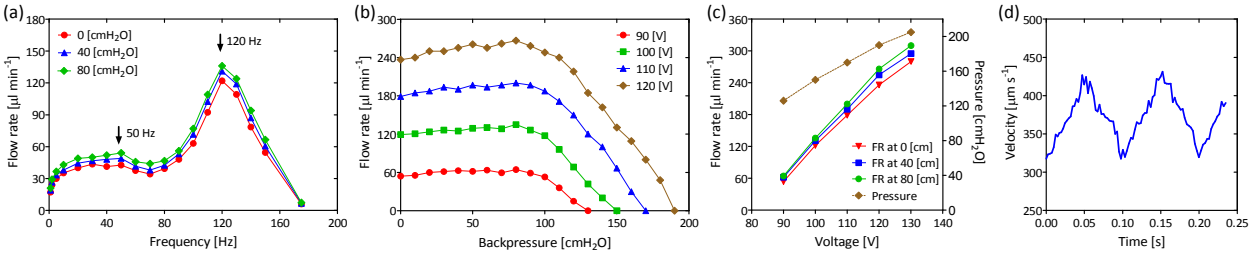

Fig. 2 (a) Flow rate as a function of the actuating frequency for three different backpressures. (b) Flow rate of the micropump as a function of backpressure for four different actuating voltages at 120 Hz. (c) Maximum flow rates (FR) and maximum pressures of the micropump as a function of the excitation voltage at 120 Hz. (d) Instantaneous velocity in the central area of a microfluidic channel as a function of time at 10 Hz and 100 V. All voltages are peak to peak.

Results and discussion

Micropump

The averaged measured flow rates as a function of the actuating frequency for three different backpressures and an actuating voltage of 100 V_{pp} (volts peak to peak) are shown in Fig. 2a. Two main resonant frequencies were observed at approximately 50 Hz and 120 Hz respectively; at 120 Hz the flow rate is maximum.

Fig. 2b shows the averaged measured flow rates of the pump as a function of backpressure for four different actuating voltages at the resonant actuating frequency of 120 Hz. We can see that the flow rate is kept fairly constant when the backpressure is lower than approximately 100 cmH_2O. However, flow rate slightly increases (approximately a 10% from zero backpressure) with increasing backpressure up to approximately 80 cmH_2O. Fig. 2b also shows that, as expected, the larger the excitation voltage, the larger the flow rate.

The maximum measured average flow rates (at three different backpressures) and the maximum measured average pressures (at zero flow rate) of the micropump as a function of the actuating voltage at 120 Hz are shown in Fig. 2c. In this figure we have another graphical representation of the increase of the flow rate with increasing backpressure. Voltages higher than 135 V_{pp} were not investigated due to potential damage to the piezoelectric actuator. Voltages lower than 85 V_{pp} do not yield repeatable results. Average flow rates between 60 µl min^{-1} and 310 µl min^{-1} can be obtained by varying the voltage between 90 V_{pp} and 130 V_{pp} with a driving frequency of 120 Hz. Lower flow rates (17 µl min^{-1}) can be obtained if the pump is operated at minor frequencies (1 Hz). If continuous periodic flow is not needed, the micropump can be pulse modulated and sub µl min^{-1} flow rates can be easily obtained. These values fall within the same orders of magnitude of similar reported micropumps.[10-13]

Fig. 2d shows the instantaneous velocity (IV) in the central area of a microchannel obtained from the µPIV measurements as a function of time. We can see that the IV varies periodically and corresponds quite well with the excitation frequency. Since flow rate is proportional to velocity we can infer that the flow rate will be pulsatile as well, presenting a similar temporal profile. Due to technological limitations of our equipment, it was not possible to measure the velocity profiles at the resonant frequency of 120 Hz.

The coefficient of variation in all the measured outlet characteristics among the tested micropumps is approximately ±15%. We believe that this relatively high value could be mainly due to two factors: drifts in fabrication inherent to a low-cost piezoelectric diaphragm[24] and drifts in positioning and gluing of the piezoelectric diaphragm.

The micropump is self-priming and tolerant to bubbles and small particles. It was able to maintain the flow rate when injecting bubbles (after a transient) or when pumping a solution of 5 µm diameter polystyrene beads in MilliQ water. The device is also robust: the micropump was left to run pumping MilliQ water at 90 V_{pp} and 120 Hz and no damage or significant changes in outlet characteristics were observed after 72 hours of continuous operation at zero backpressure. A video of the micropump running and demonstrating self-priming capability with a solution of red food dye and water can be found in the ESI.†

The micropump footprint as an independent device is small: 22 x 11 x 2.2 mm^3. This value is in the same size range of other reported backpressure independent micropumps.[10-13] However, if the pump is to be integrated in a device, the pump module requires a smaller area (inlet and outlet connection ports are avoided). Moreover, the presented device is fully compatible with the fabrication methods of laminated PMMA LOC devices, which allows straightforward on-chip integration as demonstrated in the following section.

Micropump integration example: micromixer

Mixing devices are widely used by the LOC community, therefore we chose a classic and extensively studied device, such as the sequential injection micromixer,[25,26] to demonstrate chip integration capability and applicability of our micropump. To construct the micromixer, two independent micropumps were embedded within a laminated PMMA microfluidic chip fabricated by CNC micromilling. The chip contains a T-junction and an expansion chamber (Fig. 3) so as to enhance the Taylor–Aris dispersion effect.[27] The chip was running a sequential injection mixing process between a solution of red food dye and water with a 1:1 switching ratio and a switching frequency of 2.5 Hz. The switching ratio and switching frequency are obtained by modulating the pulse width of a carrier signal (90 V_{pp} and 100 Hz) applied to each piezoelectric diaphragm. The characteristic "bands" of this process can be seen in the expansion chamber (Fig. 3a). Fig. 3b

View Article Online
DOI: 10.1039/C5RA08819D

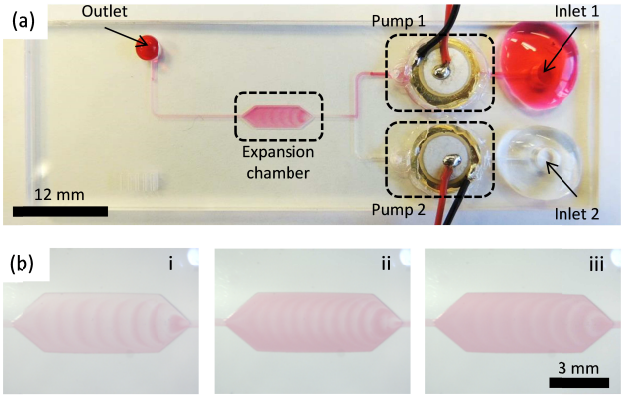

Fig. 3 (a) Photograph of the micromixer chip running a sequential injection mixing process between red food dye and water. (b) Expansion chamber snapshots during different mixing processes: i) 2:1 ratio (water : dye) at 3.33 Hz, ii) 1:1 ratio at 5 Hz and iii) 1:2 ratio at 3.33 Hz. In all cases the excitation voltage is 90 Vpp.

shows snapshots of the expansion chamber at different switching ratios and switching frequencies. Videos of the micromixer working at different switching frequencies and ratios can be found in the ESI.†

As demonstrated with this example, one or more micropumps can easily be integrated within the fabrication process of laminated PMMA microfluidic chips and effectively perform operations that require independent pumping. Although some other displacement and dynamic pumping devices[1-4,28-31] have demonstrated chip integration, smaller footprint and even backpressure independence, the presented system has several advantages: *i*) off-chip infrastructure to control piezoelectric device is generally simple, cheap and portable, *ii*) all fabrication steps can be performed with standard machine shop equipment (no clean room needed) and *iii*) the system design is scalable and compatible with many other thermoplastic and thermosetting polymers and fabrication technologies.[32]

Conclusions

A polymer chip-integrable piezoelectric micropump with low backpressure dependence was presented. The micropump is capable of pumping fluids in a periodic or pulsed fashion, yielding flow rates from sub-µl min^{-1} up to hundreds of µl min^{-1}. The flow rate is kept nearly constant up to approximately 100 cmH_2O (~10 kPa) of pressure; however maximum achievable pressures can be as high as 205 cmH_2O (~20 kPa). These characteristics are comparable and even better than several of the reported micropumps, making it suitable for many microfluidic applications.

The design of the pump enables straightforward embeddability within laminated PMMA LOC devices without the need of complex chemical-assisted methods. The fabrication technologies chosen for the micropump are ideal for prototyping and small scale production. However, pump design is compatible with large-scale manufacturing technologies that allow potential use of the micropump in low-cost disposable polymeric LOC devices.

References

1 D. J. Laser and J. G. Santiago, *J. Micromech. Microeng.*, 2004, **14**, 35-64.
2 P. Woias, Sensor. Actuat. *B-Chem.*, 2005, **105**, 28-38.
3 A. K. Au, H. Lai, B. R. Utela and A. Folch, *Micromachines*, 2011, **2**, 179-220.
4 N. T. Nguyen, X. Huang and T. K. Chuan, *J. Fluids Eng.*, 2002, **124**, 384-392.
5 D. Accoto, M. C. Carrozza and P. Dario, *J. Micromech. Microeng.*, 2000, **10**, 277-281.
6 K. -P. Kamper, J. Dopper, W. Ehrfeld and S. Oberbeck, *Proc. 11th IEEE Micr. Elect.*, 1998, 432-437.
7 J. Ni, F. Huang, B. Wang, B. Li, Q. J. Lin, *J. Micromec.h Microeng.*, 2010, **20**, 095033.
8 Bartels Mikrotechnik GmbH, Dortmund, Germany, www.bartels-mikrotechnik.de (accessed March 2015).
9 Dolomite Microfluidics, Royston, United Kingdom, www.dolomite-microfluidics.com (accessed March 2015).
10 *US Pat.*, 5 224 843 A, 1993.
11 D. Maillefer, S. Gamper, B. Frehner, P. Balmer, H. van Lintel and P. Renaud, *Proc. 14th IEEE Micr. Elect.*, 2001, 413-417.
12 G. -H. Feng and E. S. Kim, *J. Micromech. Microeng.*, 2004, **14**, 429-435.
13 A. Geipel, A. Doll, P. Jantscheff, N. Esser, U. Massing, P. Woias and F. Goldschmidtboeing, *J. Micromech. Microeng.*, 2007, **17**, 949-959.
14 T. Q. Truong and N. T. Nguyen, *J. Micromech. Microeng.*, 2004, **14**, 632-638.
15 W. Zhang, S. Lin, C. Wang, J. Hu, C. Li, Z. Zhuang, Y. Zhou, R. A. Mathies and C. J. Yang., *Lab Chip*, 2009, **9**, 3088-3094.
16 A. G. G. Toh, Z. F. Wang and S. H. Ng, 2008, arXiv:0805.0885.
17 H. Y. Tan, W. K. Loke and N. T. Nguyen, *Sensor. Actuat. B-Chem.*, 2010, **151**, 133-139.
18 P. Gu, K. Liu, H. Chen, T. Nishida and Z. H. Fan, *Anal. Chem.*, 2011, **83**, 446-452.
19 J. J. Loverich, I. Kanno and H. Kotera, *Lab Chip*, 2006, **6**, 1147-1154
20 I. D. Johnston, M. C. Tracey, J. B. Davis and C. K. L. Tan, *Lab Chip*, 2005, **5**, 318-325.
21 A. J. Conde, M. Batalla, B. Cerda, O. Mykhaylyk, C. Plank, O. Podhajcer, J. M. Cabaleiro, R. E. Madrid and L. Policastro, *Lab Chip*, 2014, **14**, 4506-4512.
22 D. Sabourin, M. Dufva, T. Jensen, J. Kutter and D. Snakenborg, *J. Micromech. Microeng.*, 2010, **20**, 037001.
23 S. Devasenathipathy, J. G. Santiago, S. T. Wereley, C. D. Meinhart and K. Takehara, *Exp. Fluids*, 2003, **34**, 504-514.
24 A.G S. B. Neto, A.M.N. Lima, F. Tejo, C. Precker and C.S. Moreira, Proc. COMSOL Conference, Boston, 2012.
25 C. K. L. Tan, M. C. Tracey, J. B, Davis and I. D. Johnston, *J. Micromech. Microeng.*, 2005, **15**, 1885-1893.
26 A Review on Mixing in Microfluidics. Y. K. Suh and S. Kang, *Micromachines*, 2010, **1**, 82-111.
27 J. T. Coleman and D. Sinton, *Microfluid. Nanofluid.*, 2005, **1**, 319-327.
28 M. A. Unger, H. P. Chou, T. Thorsen, A. Scherer and S. R. Quake, *Science*, 2000, **288**, 113-116.
29 C. Zhao and C. Yang, *Microfluid. Nanofluid.*, 2012, **13**, 179-203.
30 M. Stubbe and J. Gimsa, *Colloids Surf. A.*, 2011, **376**, 97-101.
31 A. Salari, M. Navi and C. Dalton, *Biomicrofluidics*, 2015, **9**, 014113.
32 C.-W. Tsao and D. L. DeVoe, *Microfluid. Nanofluid.*, 2009, **6**, 1-16.